



OPEN ACCESS

EDITED BY

Wei Li,
South China Sea Institute of Oceanology
(CAS), China

REVIEWED BY

Xiting Liu,
Ocean University of China, China
Tao Yang,
Nanjing University, China

*CORRESPONDENCE

Xudong Wang
✉ xd-wang@shou.edu.cn

SPECIALTY SECTION

This article was submitted to
Marine Biogeochemistry,
a section of the journal
Frontiers in Marine Science

RECEIVED 16 March 2023

ACCEPTED 10 April 2023

PUBLISHED 20 April 2023

CITATION

Feng X, Jia Z and Wang X (2023)
Uncovering the temporal carbon isotope
($\delta^{13}\text{C}$) heterogeneity in seep carbonates: a
case study from Green Canyon, northern
Gulf of Mexico.
Front. Mar. Sci. 10:1187594.
doi: 10.3389/fmars.2023.1187594

COPYRIGHT

© 2023 Feng, Jia and Wang. This is an open-
access article distributed under the terms of
the [Creative Commons Attribution License
\(CC BY\)](https://creativecommons.org/licenses/by/4.0/). The use, distribution or
reproduction in other forums is permitted,
provided the original author(s) and the
copyright owner(s) are credited and that
the original publication in this journal is
cited, in accordance with accepted
academic practice. No use, distribution or
reproduction is permitted which does not
comply with these terms.

Uncovering the temporal carbon isotope ($\delta^{13}\text{C}$) heterogeneity in seep carbonates: a case study from Green Canyon, northern Gulf of Mexico

Xia Feng¹, Zice Jia² and Xudong Wang^{2*}

¹Guangdong Polytechnic of Environmental Protection Engineering, Foshan, Guangdong, China,

²Shanghai Engineering Research Center of Hadal Science and Technology, College of Marine Sciences, Shanghai Ocean University, Shanghai, China

Authigenic carbonates that form at hydrocarbon seeps, known as seep carbonates, are direct records of past fluid flow close to the seafloor. Stable carbon isotopes of seep carbonates ($\delta^{13}\text{C}_{\text{carb}}$) have been widely used as a proxy for determining fluid sources and seepage mode. Although the spatial heterogeneity of $\delta^{13}\text{C}$ in seep carbonates is increasingly understood, the temporal heterogeneity of $\delta^{13}\text{C}$ in seep carbonates is not well studied. In this study, we report $\delta^{13}\text{C}$ values of different components (clasts, matrix, and pore-filling cements) for 124 subsamples drilled across an authigenic carbonate block from Green Canyon block 140 (GC140) of the northern Gulf of Mexico continental slope. High-Mg calcite is the dominant mineral regardless the types of components. The $\delta^{13}\text{C}_{\text{carb}}$ values range from -39.6% to 3.6% , indicating multiple dissolved inorganic carbon (DIC) sources that include methane carbon (^{13}C -depleted), seawater DIC, and residual CO_2 from methanogenesis (^{13}C -enriched). Specifically, the clasts show large variability in $\delta^{13}\text{C}$ values (-39.6% to 2.3% ; mean: -27.6% , $n = 71$), demonstrating the dominance of methane-derived fluids during formation at the initial seepage stage. The $\delta^{13}\text{C}$ values of the matrix vary between -29.4% and 3.4% (mean: -11.6% , $n = 21$). The carbon isotopes of pore-filling cements that formed most recently vary narrowly, with $\delta^{13}\text{C}$ values of -3.2% to 3.6% (mean: 1.7% , $n = 28$). Isotopic variations within individual samples were observed in seep carbonate. However, common trends occur across components of carbonates that formed during different seepage stages. This suggests that the temporal evolution of local fluid sources may play an important role in determining carbonate isotope geochemistry. Studies regarding seeps must take into account the highly variable fluids that leave their geochemical imprints on the seep carbonate.

KEYWORDS

hydrocarbon seep, methane, authigenic carbonate, stable carbon isotopes, Gulf of Mexico

1 Introduction

Observations of methane seepage in marine settings are common (Suess, 2020, and references therein). The seeping methane is primarily consumed by consortia of methane-oxidizing archaea and sulfate-reducing bacteria, a process known as anaerobic oxidation of methane (e.g., Boetius et al., 2000). As a result, carbonate alkalinity increase induces the precipitation of carbonate minerals close to the seafloor. These carbonates serve as an excellent archive of past seepage (Ritger et al., 1987; Bohrmann et al., 1998; Aloisi et al., 2000; Peckmann et al., 2001; Mazzini et al., 2004; Gontharet et al., 2007; Naehr et al., 2007; Haas et al., 2010; Sun et al., 2015; Himmler et al., 2019; Wang et al., 2022).

Carbon isotopes in the mineral phase of seep carbonate are derived from ambient bicarbonate and dissolved inorganic carbon (DIC). The variation of carbon isotopic composition of these carbonates (as much as 85‰) indicating an almost equally wide range of geochemical processes involved in carbonate precipitation (e.g., Naehr et al., 2007). The stable carbon isotopes of seep carbonates ($\delta^{13}\text{C}_{\text{carb}}$) have been widely used since the discovery of methane seep in 1980s for almost any carbonate-based seep studies. For instance, $\delta^{13}\text{C}$ values provided stable isotopic evidence for methane seeps in Neoproterozoic postglacial cap carbonates (Jiang et al., 2003), demonstrated the involvement of oil seepage (Smrzka et al., 2016; Sun et al., 2020), meteoric water and methogenesis during carbonate formation (Naehr et al., 2007).

Seep carbonates are known to show a wide range of carbon isotopic and variation across multiple geographic areas (Gontharet et al., 2007; Roberts et al., 2010; Zhang et al., 2023). The observed variations, spatial heterogeneity of $\delta^{13}\text{C}$ in seep carbonates, mainly reflect local controls on the sources of fluids and flux of the fluids, which have been well constrained. In contrast, carbon isotopic variation in authigenic carbonate composition within individual study samples, the temporal heterogeneity of $\delta^{13}\text{C}$ in seep carbonates is not well studied. Such temporal heterogeneity of $\delta^{13}\text{C}$ in seep carbonates can be used to constrain the evolution of

the fluid sources and mode of seepage with time. Given that seep-related authigenic minerals provide an important geological archive, as they represent one of the few permanent records of an otherwise ephemeral phenomenon (Roberts et al., 2010; Smrzka et al., 2016; Chen et al., 2019).

The aim of this paper is to assess the heterogeneity of $\delta^{13}\text{C}$ in a single seep carbonate sample to reveal the evolution of seep fluids during carbonate formation. We describe different types of components of the studied carbonates including clasts, matrix, and pore-filling cements that represent archive of variation between different formation stages. We use the obtained data to constrain the conditions under which carbonate formation occurred and uncover the temporal carbon isotope heterogeneity during the precipitation.

2 Samples and methods

2.1 Samples

The Green Canyon block 140 (GC140) seep site is in the northern upper continental slope of the GOM (Figure 1; Roberts et al., 1989; Roberts and Feng, 2013). Bathymetric and high-resolution seismic profiles and side-scan sonographs indicate that the thin sedimentary sequence over the shallow salt mass of site GC140 is broken by numerous faults and that most mounded carbonates are cut due to salt deformation (Roberts and Carney, 1997; Roberts et al., 2000). Previous investigations revealed the occurrence of mound-like buildups, 20–100 m in diameter and up to 20 m in height, are composed of chaotically oriented carbonate blocks in the surrounding sediments (Roberts et al., 1990; Roberts and Aharon, 1994; Roberts et al., 2000; Roberts et al., 2010; Roberts and Feng, 2013). In terms of the seepage, the site GC140 is currently not active. However, scattered living tube worms and sponges were present at the sampling site (Roberts et al., 2010). The studied authigenic carbonate was recovered during Pisces II dive in 1989

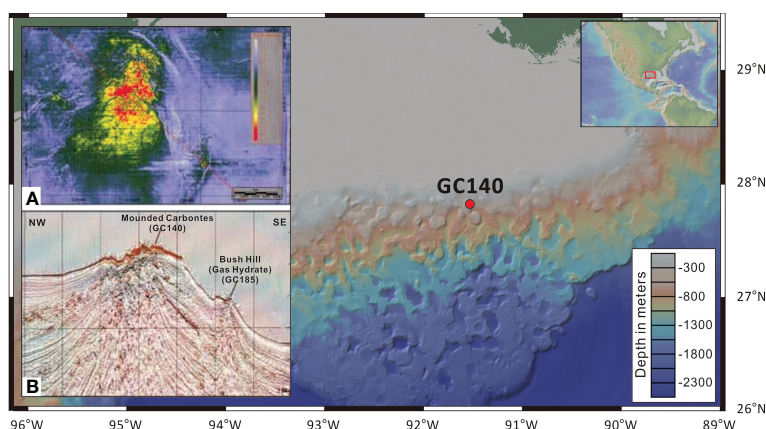


FIGURE 1

Location of the Green Canyon block 140 (GC140; 27°48'N/91°32'W) study site, northern Gulf of Mexico (from Bian et al., 2013). The inset 3-D seismic surface amplitude illustrates the extent of the hard bottom (A) and the profile view (B), showing that the dome top has an irregular surface and that the seafloor reflector is a strong, positive reflector, indicating a hard bottom (Roberts, 2001).

(Roberts et al., 1989). The sample was collected from the seafloor. The water depth at the site was 320 m, and the bottom water temperature was about 13°C (Roberts et al., 2010).

2.2 Methods

After collection, the sample was rinsed with fresh water and left to air dry. The resulting carbonate block was photographed digitally and then cut into slabs using a water-lubricated rock saw. Each slab was also photographed. Visual examination of the rock slab used to distinguish main components of the carbonate (see Figure 2), which were determined to be clasts, matrix, and pore-filling cements. All components were collected using a dental drill to determine their mineralogy. Mineralogy was determined using x-ray diffraction (XRD) using a Rigaku DXR 3000 computer-automated diffractometer at the Guangzhou Institute of Geochemistry, Chinese Academy of Sciences (CAS). Bulk samples were powdered to less than 200 mesh. The x-ray source operated at 40 kV and 40 mA using CuK α radiation equipped with a diffracted beam graphite monochromator. Scans were made through a 5-65° using a 0.02° step at 5 sec/step.

Subsamples for carbonate carbon and oxygen isotopes were extracted from polished rock slabs using a hand-held dental drill. Clast, matrix, and pore-filling cements were selected for sampling (see Figure 2 for sampling locations). The powdered samples were processed with 100% phosphoric acid at 70°C to release CO₂ for analysis using a Delta V Advantage stable isotopic mass spectrometer at Shanghai Ocean University. All isotope values are expressed using the δ -notation relative to the Vienna-Pee Dee Belemnite (V-PDB) standard. The values were reported in permil (‰) with a standard deviation of less than 0.1‰ (2 σ) for both $\delta^{13}\text{C}$ and $\delta^{18}\text{O}$ values.

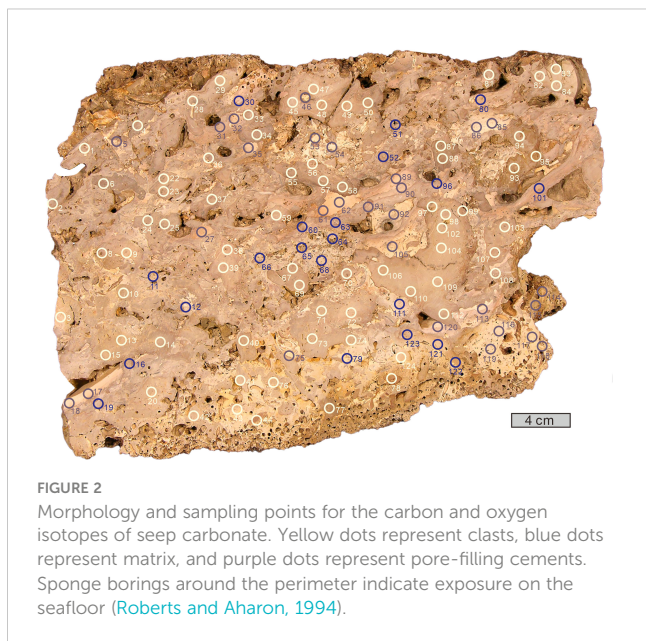


FIGURE 2
Morphology and sampling points for the carbon and oxygen isotopes of seep carbonate. Yellow dots represent clasts, blue dots represent matrix, and purple dots represent pore-filling cements. Sponge borings around the perimeter indicate exposure on the seafloor (Roberts and Aharon, 1994).

3 Results

3.1 Mineralogy and petrography

The carbonate sample show no obvious stratification and present as irregular structures. The mineral composition of the carbonate is summarized in Table 1. Visual examination of the rock slab revealed that the carbonate consisted mainly of clasts, carbonate mud matrix, and pore-filling cements (Figure 2). The paragenetic sequence identified in this study consisted of three stages: (1) deposition of carbonate clasts; (2) precipitation of microcrystalline matrix and (3) pore-filling cements. High-Mg calcite serves as the predominant mineral while a small amount (less than 3%) of quartz is present for all components. The clasts occur as homogeneous micrite while the matrix and pore-filling cements are characterized by a dominance of microcrystalline Mg-calcite. Geopetal structures in various orientations are common, suggesting multiple attitudes during the development (Roberts, 2001). Sponge borings around the perimeter indicate exposure on the seafloor (Roberts and Aharon, 1994).

3.2 Carbonate carbon and oxygen isotopes

The carbon and oxygen isotopic compositions of the three main types of components vary widely (Table 2; Figure 3). The $\delta^{13}\text{C}_{\text{carb}}$ values of the clasts vary between -39.6‰ to 2.3‰ (mean: -27.6‰ , $n = 71$). The $\delta^{13}\text{C}_{\text{carb}}$ values of the matrix are from -29.4‰ to 3.4‰ (mean: -11.6‰ , $n = 21$). The carbon isotopes of pore-filling cements vary narrowly with $\delta^{13}\text{C}_{\text{carb}}$ values between -3.2‰ and 3.6‰ (mean: 1.7‰ , $n = 28$). In contrast, the stable oxygen isotopic compositions of these components display relatively narrow ranges, with $\delta^{18}\text{O}$ values from 1.9‰ to 4.1‰ (mean: 3.3‰ , $n = 71$) for clasts, 1.8‰ to 3.9‰ (mean: 2.9‰ , $n = 21$) for the matrix, and 2.4‰ to 4.1‰ (mean: 3.2‰ , $n = 28$) for the pore-filling cements.

4 Discussion

4.1 Implications on megascopic characteristics and mineral composition of the carbonate

Seep carbonates have significant potential for preserving detailed information on the paleoenvironmental conditions of their formation (Haas et al., 2010; Oppo et al., 2017; Oppo et al., 2020). The megascopic features of the studied carbonate reflect local controls, such as the intensity and duration of seep activity at the formation site. The block is heterogeneous, up to $0.5 \times 0.5 \times 0.5$ m (length, width and height), represent the biggest carbonate sample obtained from the Gulf of Mexico (Figure 2; Roberts and Feng, 2013). At a small scale, the carbonate consists of clasts that formed initially, followed by the matrix, these were then cemented by pore-filling cements (Figure 2), indicating multiple stages during the formation of the carbonate. A previous study on samples from the

TABLE 1 Mineral composition of the seep carbonate.

Test ID	High-Mg calcite (%)	Aragonite (%)	Quartz (%)	Comment
47	97.8		2.6	Matrix
67	98.2		1.8	
106	97.5		2.5	
60	98.9		1.1	Clast
101	98.9		1.1	
18	100			Pore-filling cement
61	99.3		0.7	
86	79.1	19.8	1.1	

Sample locations are indicated in Figure 2.

TABLE 2 Stable carbon and oxygen isotopic compositions of the seep carbonate.

Test ID	$\delta^{13}\text{C}$ (‰,VPDB)	$\delta^{18}\text{O}$ (‰,VPDB)	Comment
1	-1.3	3.6	Clast
2	-34.9	3.4	Clast
3	-18.3	3.7	Clast
4	-30.6	3.2	Clast
5	1.7	3.5	Pore-filling cement
6	-34.4	3.4	Clast
8	-25.3	3.6	Clast
9	-24.4	3.5	Clast
10	-24.2	3.8	Clast
11	-16.3	3.5	Matrix
12	-20.4	2.8	Matrix
13	-19.9	3.5	Clast
14	-32.4	2.7	Clast
15	-22.2	3.5	Clast
16	-11	3.9	Matrix
17	3.2	3.3	Pore-filling cement
18	0.4	4.1	Pore-filling cement
19	-3.1	3.5	Matrix
20	-22.3	3.3	Clast
22	-34.8	3.4	Clast
23	-33.3	3.3	Clast
24	-36.9	3.4	Clast
25	-31.6	2.3	Clast
27	3	3.6	Pore-filling cement
28	-34.2	3.3	Clast

(Continued)

TABLE 2 Continued

Test ID	$\delta^{13}\text{C}$ (‰,VPDB)	$\delta^{18}\text{O}$ (‰,VPDB)	Comment
29	-33	3.1	Clast
30	-6.5	1.8	Matrix
31	1.4	2.9	Pore-filling cement
32	3.5	3.3	Pore-filling cement
33	-29.6	3.3	Clast
34	-28.8	3.3	Clast
35	3.3	2.4	Pore-filling cement
36	-13.8	3.2	Clast
37	-32.5	3.3	Clast
38	-17.9	3.4	Clast
39	-17.4	3.4	Clast
40	-25.1	3.3	Clast
41	-32.6	2.6	Clast
42	-29.7	3.6	Clast
43	-26.7	2.8	Clast
44	-27.5	3.3	Clast
45	-34.2	3.2	Clast
46	-0.3	3.4	Pore-filling cement
47	-33.6	3.4	Clast
48	-32.2	3.2	Clast
49	-30	3.2	Clast
50	-32.6	3.2	Clast
51	-1.5	2.8	Matrix
52	-18	3	Matrix
53	0.5	3.2	Pore-filling cement
54	-2.7	3.3	Pore-filling cement
55	-35.3	3.3	Clast
56	-29.4	3.5	Clast
57	-36.7	3.3	Clast
58	-36.9	3.4	Clast
59	2.3	3.2	Clast
60	-7.7	3.1	Matrix
61	2.3	3.2	Pore-filling cement
62	3.4	3.7	Pore-filling cement
63	-0.9	3	Matrix
64	-20.7	2.4	Matrix
65	-9.9	3.7	Matrix
66	-22.6	3.7	Matrix
67	-31.3	3.9	Clast

(Continued)

TABLE 2 Continued

Test ID	$\delta^{13}\text{C}$ (‰,VPDB)	$\delta^{18}\text{O}$ (‰,VPDB)	Comment
68	-10.9	3	Matrix
69	-33.6	2.8	Clast
70	-34.9	3.5	Clast
71	-15.5	3.2	Clast
72	-17.3	3.5	Clast
73	-18.8	3.2	Clast
74	-33	3.7	Clast
75	-3.2	3.5	Pore-filling cement
76	-27.7	2	Clast
77	-26.7	3.2	Clast
78	-28.1	3.9	Clast
79	-10.7	3.1	Matrix
80	2.5	3.5	Matrix
81	-9.7	3.3	Clast
82	-36	2.3	Clast
83	-36	3.5	Clast
84	-34.8	3.4	Clast
85	1.8	3.5	Pore-filling cement
86	1.2	3.5	Pore-filling cement
87	-2.6	4.1	Clast
88	-4.2	3.4	Clast
89	3.6	3.8	Pore-filling cement
90	-0.3	3.6	Pore-filling cement
91	1.9	3.6	Pore-filling cement
92	3.2	2.9	Pore-filling cement
93	-38	3.5	Clast
94	-37.5	3.2	Clast
95	-32.5	4	Clast
96	2.5	1.9	Matrix
97	-27.8	3.7	Clast
98	-39.6	3.3	Clast
99	-35.3	3.6	Clast
101	3.4	2.3	Matrix
102	-37.8	3.4	Clast
103	-33.3	3	Clast
104	-37.3	3.3	Clast
105	2.1	3.4	Pore-filling cement
106	-33.4	3.4	Clast
107	-35.4	1.9	Clast

(Continued)

TABLE 2 Continued

Test ID	$\delta^{13}\text{C}$ (‰,VPDB)	$\delta^{18}\text{O}$ (‰,VPDB)	Comment
108	-3.4	3	Clast
109	-30.9	3.1	Clast
110	-34.3	2.8	Clast
111	-10.3	1.9	Matrix
112	-9.3	3	Clast
113	2.7	2.9	Pore-filling cement
114	1.9	2.7	Pore-filling cement
115	1.9	3	Pore-filling cement
116	1.9	3.1	Pore-filling cement
117	1.4	2.7	Pore-filling cement
118	1.5	2.4	Pore-filling cement
119	1.8	3.2	Pore-filling cement
120	3.4	3.3	Pore-filling cement
121	-29.4	2.2	Matrix
122	-28.8	2.8	Matrix
123	-23.7	3.3	Matrix
124	-27.9	2.7	Clast

Sample locations are indicated in Figure 2.

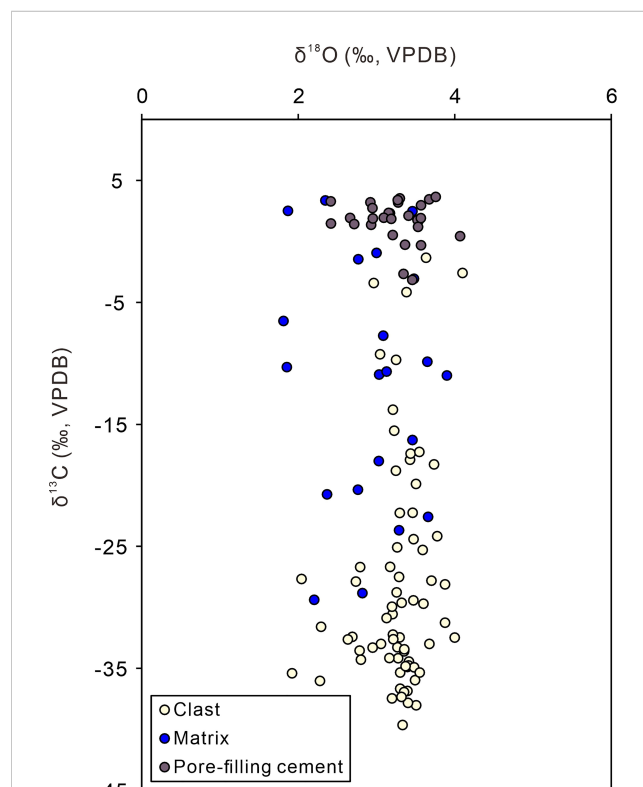


FIGURE 3 Stable carbon and oxygen isotopic compositions of seep carbonate.

same site identified three types of carbonates with ^{14}C ages from 46.5 ka to 11.7 ka BP (Bian et al., 2013). The observed geopetal structures with different orientations in the carbonate indicate multiple reworking, most likely resulting from salt tectonics in this area (Roberts, 2001; Figure 2).

The precipitation of carbonate is related to the presence of rising methane-rich fluids, which migrate upward through faults (Figure 1; Roberts and Feng, 2013). The predominance of high-Mg calcite and the negligible content of background sediment (< 3% quartz) in the seep carbonate suggests that the carbonate precipitated in sediment (Table 1; Gontharet et al., 2007). As suggested by numerous studies, high-Mg calcite formation occurs in a deep sediment column with relatively low sulfate content (Burton, 1993; Greinert et al., 2001; Bayon et al., 2007; Haas et al., 2010).

4.2 Constraints on the temporal $\delta^{13}\text{C}$ heterogeneity in seep carbonate

The authigenic minerals in cold seeps help to reveal the chemistry of the diagenetic fluids. The oxygen isotope composition of seep carbonates is commonly a convolution of multiple variables, such as temperature, fluid source, pH and growth rate (Watkins et al., 2014). In this study, the oxygen isotope compositions fall within the typical range of seep carbonate in the Gulf of Mexico (Roberts et al., 2010). The variation of carbon isotope in seep carbonate is basically controlled by the mixability of different carbon sources (Gontharet et al., 2007). The extremely large variable range of $\delta^{13}\text{C}_{\text{carb}}$ values (from -39.6‰ to 3.6‰ ; Figure 3) of the sample reveal that multiple DIC sources were involved during the precipitation of the carbonate. At GC140 seep site, potential carbon sources include: 1) methane ($\delta^{13}\text{C} = -110\text{‰}$ to -30‰ ; Whiticar et al., 1986; Whiticar, 1999), 2) crude oil fraction ($\delta^{13}\text{C} = -35\text{‰}$ to -25‰ ; Roberts and Aharon, 1994), 3) seawater ($\delta^{13}\text{C} = 0 \pm 3\text{‰}$; Anderson and Arthur, 1983), and 4) residual CO_2 from methanogenesis ($\delta^{13}\text{C}$ as high as 26‰ ; Paull et al., 2007). The lowest $\delta^{13}\text{C}_{\text{carb}}$ value of -39.6‰ suggest that methane is the primary carbon source, while the highest $\delta^{13}\text{C}_{\text{carb}}$ value of 3.6‰ points to the possible contribution of residual CO_2 from methanogenesis (cf. Bian et al., 2013). Although significant isotopic variations were observed within individual samples, the scattered distribution of the $\delta^{13}\text{C}_{\text{carb}}$ values makes it challenging to determine the DIC source based solely on carbon isotopes.

Nevertheless, the variation in $\delta^{13}\text{C}_{\text{carb}}$ values among different seepage stages of carbonate formation suggests a shift in dominant carbon sources. The relatively more negative carbon isotopic ratios (from -39.6‰ to 2.3‰ ; mean: -27.6‰ , $n = 71$) of the clasts indicate that methane is the primary carbon source. The moderately negative $\delta^{13}\text{C}_{\text{carb}}$ values (from -29.4‰ to 3.4‰ ; mean: -11.6‰ , $n = 21$) of the matrix likely reflect less incorporation of methane-derived DIC compared to clasts due to a decrease in seepage intensity. The $\delta^{13}\text{C}_{\text{carb}}$ values close to 0 of the pore-filling cement

(from -3.2‰ to 3.6‰ ; mean: 1.7‰ , $n = 28$) likely result from the incorporation of seawater DIC due to the cessation of seepage. The contribution of DIC from residual CO_2 from methanogenesis cannot be ruled out but the contribution should not be significant. The $\delta^{13}\text{C}_{\text{carb}}$ values of clast, matrix, and pore-filling cements that formed during different seepage stages provide insight into the temporal evolution of local fluid sources at site GC140.

4.3 A time-capsule $\delta^{13}\text{C}_{\text{carb}}$ of seep system

In the Gulf of Mexico (GOM), the deformation of salt bodies and faults results in dynamic fluid flow, leading to rapid expulsion of fluid and gas. This process creates conditions that are favorable for the formation of authigenic carbonates in close proximity to the seafloor (Roberts, 2001; Roberts, 2011). The carbonate outcropping at the seafloor provides an accessible overview to monitor the long-term dynamics of fluid and gas expulsions. By integrating mineralogical and geochemical data, a schematic model of the evolution of seep fluids at site GC140 is proposed (Figure 4; Bian et al., 2013).

During stage I, high flux fluid flow induced the formation of clasts in the subsurface sediments. The high methane flux resulted in relatively negative $\delta^{13}\text{C}$ values of the carbonates (Luff and Wallmann, 2003; Peckmann and Thiel, 2004). In stage II, low flux of fluid seepage at the studied site led to the formation of the matrix and voids. The previously formed clasts were cemented together by a surrounding matrix sediment and left voids during this stage. In stage III, fluid seepage decreased, and the formation of pore-filling cements tended to occur. At the same time, seawater was transported downwards from a minor mode to a moderate mode (Figure 4).

It is noteworthy that during all three stages, salt tectonics, such as salt bodies and salt diapirs, developed in the study site (Cook and D'Onfro, 1991; Sassen et al., 1999). Green Canyon is underlain by a Neogene salt weld (Seni, 1992). Submersible observations and high-resolution acoustic datasets show that faults are widespread in sediments as a result of tectonic activity (Roberts et al., 1990; Roberts et al., 1993; Roberts et al., 2000), suggesting that the movement of salt has been active (Bian et al., 2013).

5 Conclusions

The carbonate block obtained from site GC140 in the northern Gulf of Mexico has provided valuable insights into the significant $\delta^{13}\text{C}$ heterogeneity (over 40‰) observed in a single seep carbonate sample. The $\delta^{13}\text{C}$ values ranged from -39.6‰ to 2.3‰ (mean: -27.6‰ , $n = 71$) for clasts, from -29.4‰ to 3.4‰ (mean: -11.6‰ , $n = 21$) for matrix, and from -3.2‰ to 3.6‰ (mean: 1.7‰ , $n = 28$) for the pore-filling cements. These variations suggest that multiple dissolved inorganic carbon (DIC) sources contributed to the formation of different components of the carbonate at different stages. The temporal evolution of local fluid sources may have

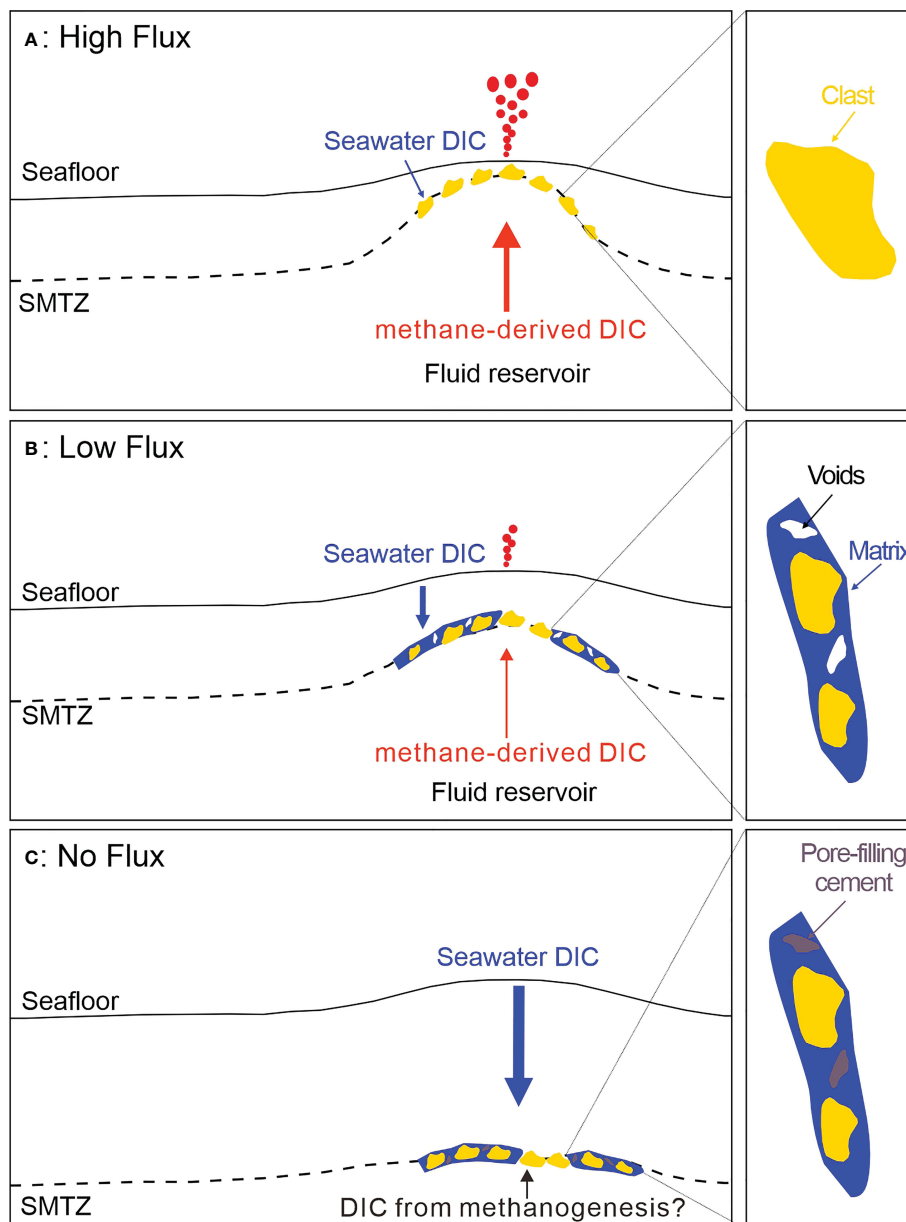


FIGURE 4

Schematic model illustrating the evolution of seep fluids and formed components of the seep carbonate (after Feng et al., 2009 and Bian et al., 2013). (A) High flux of the fluid seepage led to precipitation of clasts in subsurface sediment; (B) The clasts were being cemented together by a surrounding matrix sediment during the decrease of fluid flux. (C) Pore-filling cements tend to occur then the fluid flux diseased. Meantime, seawater was transported downwards from a minor mode to moderate mode. SMTZ, sulfate methane transition zone. The arrow sizes are proportional to the upward methane fluxes and downward seawater fluxes.

played a crucial role in determining the carbonate isotope geochemistry. Therefore, the highly variable fluids that leave their geochemical imprints on seep carbonate must be considered in any seep-related studies.

Data availability statement

The original contributions presented in the study are included in the article/supplementary material. Further inquiries can be directed to the corresponding author.

Author contributions

Conceptualization: XW; methodology: XF and ZJ; formal analysis: XF and ZJ; investigation: ZJ; XW; data curation: XW; writing—original draft preparation: XF; writing—review and editing: XW; visualization: XW; supervision: XW; project administration: XW; funding acquisition: XW. All authors contributed to the article and approved the submitted version.

Funding

This study was sponsored by Shanghai Sailing Program (Grant: 21YF1416800) and by the Chenguang Program of Shanghai Education Development Foundation and Shanghai Municipal Education Commission (Grant: 22CGA58).

Acknowledgments

Sample was collected during projects funded by the U.S. Bureau of Ocean Energy Management and the National Oceanic and Atmospheric Administration's National Undersea Research Program. Harry H. Roberts (Louisiana State University) and Dong Feng (Shanghai Ocean University) are thanked for providing the sample. Yang Lu (University of Oslo) is thanked for XRD mineral identification.

References

- Aloisi, G., Pierre, C., Rouchy, J., Foucher, J., Woodside, J., and Party, M. S. (2000). Methane-related authigenic carbonates of eastern Mediterranean Sea mud volcanoes and their possible relation to gas hydrate destabilisation. *Earth Planet. Sci. Lett.* 184, 321–338. doi: 10.1016/S0012-821X(00)00322-8
- Anderson, T. F., and Arthur, M. A. (1983). "Stable isotopes of oxygen and carbon and their application to sedimentologic and paleoenvironmental problems," in *Sedimentary geology*. (Dallas: Society of economic paleontologists and mineralogists), 1–151. Available at: <https://pubs.geoscienceworld.org/sepm/books/book/1147/chapter-abstract/10572697/Stable-Isotopes-of-Oxygen-and-Carbon-and-their?redirectedFrom=PDF>.
- Bayon, G., Pierre, C., Etoubleau, J., Voisset, M., Cauquil, E., Marsset, T., et al. (2007). Sr/Ca and Mg/Ca ratios in Niger delta sediments: implications for authigenic carbonate genesis in cold seep environments. *Mar. Geol.* 241, 93–109. doi: 10.1016/j.margeo.2007.03.007
- Bian, Y., Feng, D., Roberts, H. H., and Chen, D. (2013). Tracing the evolution of seep fluids from authigenic carbonates: green canyon, northern gulf of Mexico. *Mar. Pet. Geol.* 44, 71–81. doi: 10.1016/j.marpetgeo.2013.03.010
- Boetius, A., Ravensschlag, K., Schubert, C. J., Rickert, D., Widdel, F., Gieseke, A., et al. (2000). A marine microbial consortium apparently mediating anaerobic oxidation of methane. *Nature* 407, 623–626. doi: 10.1038/35036572
- Bohrmann, G., Greinert, J., Suess, E., and Torres, M. (1998). Authigenic carbonates from the cascadia subduction zone and their relation to gas hydrate stability. *Geology* 26, 647–650. doi: 10.1130/0091-7613(1998)026<0647:ACFTCS>2.3.CO;2
- Burton, E. A. (1993). Controls on marine carbonate cement mineralogy: review and reassessment. *Chem. Geol.* 105, 163–179. doi: 10.1016/0009-2541(93)90124-2
- Chen, F., Wang, X., Li, N., Cao, J., Bayon, G., Peckmann, J., et al. (2019). Gas hydrate dissociation during sea-level highstand inferred from U/Th dating of seep carbonate from the south China Sea. *Geophys. Res. Lett.* 46, 13928–13938. doi: 10.1029/2019GL085643
- Cook, D., and D'Onfro, P. (1991). Jolliet field thrust fault structure and stratigraphy green canyon block 184, offshore Louisiana. *Trans. Gulf Coast. Assoc. Geological Soci.* 41, 100–121.
- Feng, D., Chen, D., and Peckmann, J. (2009). Rare earth elements in seep carbonates as tracers of variable redox conditions at ancient hydrocarbon seeps. *Terra. Nova.* 21, 49–56. doi: 10.1111/j.1365-3121.2008.00855.x
- Gontharet, S., Pierre, C., Blanc-Valleron, M.-M., Rouchy, J. M., Fouquet, Y., Bayon, G., et al. (2007). Nature and origin of diagenetic carbonate crusts and concretions from mud volcanoes and pockmarks of the Nile deep-sea fan (eastern Mediterranean Sea). *Deep-Sea. Res. Part II-Top. Stud. Oceanogr.* 54, 1292–1311. doi: 10.1016/j.dsr2.2007.04.007
- Greinert, J., Bohrmann, G., and Suess, E. (2001). "Gas hydrate-associated carbonates and methane-venting at hydrate ridge: classification, distribution and origin of authigenic lithologies," in *Natural gas hydrates: occurrence, distribution, and detection. geophysical monographs*, vol. 124. Eds. C. K. Paull and W. P. Dillon (Washington, DC: American Geophysical Union), 99–113.
- Haas, A., Peckmann, J., Elvert, M., Sahling, H., and Bohrmann, G. (2010). Patterns of carbonate authigenesis at the kouilou pockmarks on the Congo deep-sea fan. *Mar. Geol.* 268, 129–136. doi: 10.1016/j.margeo.2009.10.027

Conflict of interest

The authors declare that the research was conducted in the absence of any commercial or financial relationships that could be construed as a potential conflict of interest.

Publisher's note

All claims expressed in this article are solely those of the authors and do not necessarily represent those of their affiliated organizations, or those of the publisher, the editors and the reviewers. Any product that may be evaluated in this article, or claim that may be made by its manufacturer, is not guaranteed or endorsed by the publisher.

Himmler, T., Sahy, D., Martma, T., Bohrmann, G., Plaza-Faverola, A., Bünz, S., et al. (2019). A 160,000-year-old history of tectonically controlled methane seepage in the Arctic. *Sci. Adv.* 5, eaaw1450. doi: 10.1126/sciadv.aaw1450

Jiang, G., Kennedy, M., and Christie-Blick, N. (2003). Stable isotopic evidence for methane seeps in neoproterozoic postglacial cap carbonates. *Nature* 426, 822–826. doi: 10.1038/nature02201

Luff, R., and Wallmann, K. (2003). Fluid flow, methane fluxes, carbonate precipitation and biogeochemical turnover in gas hydrate-bearing sediments at hydrate ridge, cascadia margin: numerical modeling and mass balances. *Geochim. Cosmochim. Acta* 67, 3403–3421. doi: 10.1016/S0016-7037(03)00127-3

Mazzini, A., Ivanov, M. K., Parnell, J., Stadnitskaya, A., Cronin, B., Poludetkina, E., et al. (2004). Methane-related authigenic carbonates from the black Sea: geochemical characterization and relation to seeping fluids. *Mar. Geol.* 212, 153–181. doi: 10.1016/j.margeo.2004.08.001

Naehr, T. H., Eichhubl, P., Orphan, V. J., Hovland, M., Paull, C. K., Ussler, W., et al. (2007). Authigenic carbonate formation at hydrocarbon seeps in continental margin sediments: a comparative study. *Deep-Sea. Res. Part II-Top. Stud. Oceanogr.* 54, 1268–1291. doi: 10.1016/j.dsr2.2007.04.010

Oppo, D., De Siena, L., and Kemp, D. B. (2020). A record of seafloor methane seepage across the last 150 million years. *Sci. Rep.* 10, 2562. doi: 10.1038/s41598-020-59431-3

Oppo, D., Viola, I., and Capozzi, R. (2017). Fluid sources and stable isotope signatures in authigenic carbonates from the northern Apennines, Italy. *Mar. Pet. Geol.* 86, 606–619. doi: 10.1016/j.marpetgeo.2017.06.016

Paull, C. K., Ussler, W., Peltzer, E. T., Brewer, P. G., Keaten, R., Mitts, P. J., et al. (2007). Authigenic carbon entombed in methane-soaked sediments from the northeastern transform margin of the guaymas basin, gulf of California. *Deep-Sea. Res. Part II-Top. Stud. Oceanogr.* 54, 1240–1267. doi: 10.1016/j.dsr2.2007.04.009

Peckmann, J., Reimer, A., Luth, U., Luth, C., Hansen, B. T., Heinicke, C., et al. (2001). Methane-derived carbonates and authigenic pyrite from the northwestern black Sea. *Mar. Geol.* 177, 129–150. doi: 10.1016/S0025-3227(01)00128-1

Peckmann, J., and Thiel, V. (2004). Carbon cycling at ancient methane-seeps. *Chem. Geol.* 205, 443–467. doi: 10.1016/j.chemgeo.2003.12.025

Ritger, S., Carson, B., and Suess, E. (1987). Methane-derived authigenic carbonates formed by subduction-induced pore-water expulsion along the Oregon/Washington margin. *Geol. Soc. Am. Bull.* 98, 147–156. doi: 10.1130/0016-7606(1987)98<147:MACFBS>2.0.CO;2

Roberts, H. H. (2001). "Fluid and gas expulsion on the northern gulf of Mexico continental slope: mud-prone to mineral-prone responses," in *Natural gas hydrates: occurrence, distribution, and detection*. Eds. C. K. Paull and W. P. Dillon (Washington, DC, USA: American Geophysical Union), 145–161.

Roberts, H. H. (2011). "Surficial geology of the northern gulf of Mexico continental slope: impacts of fluid and gas expulsion," in *Gulf of Mexico origin, waters, and biota. geology*, 3. Eds. N. A. Buster, W. C. Holmes and D. K. Camp (Texas: Texas A&M University Press), 209–228.

Roberts, H. H., and Aharon, P. (1994). Hydrocarbon-derived carbonate buildups of the northern gulf of Mexico continental slope: a review of submersible investigations. *Geo-Mar. Lett.* 14, 135–148. doi: 10.1007/BF01203725

- Roberts, H. H., Aharon, P., Carney, R., Larkin, J., and Sassen, R. (1990). Sea Floor responses to hydrocarbon seeps, Louisiana continental slope. *Geo-Mar. Lett.* 10, 232–243. doi: 10.1007/BF02431070
- Roberts, H. H., Aharon, P., and Walsh, M. W. (1993). “Cold-seep carbonates of the Louisiana continental slope to basin floor,” in *Carbonate microfabrics: frontiers in sedimentary geology*. Eds. R. Rezak and D. L. Lavoie (New York, NY, USA: Springer-Verlag), 95–104.
- Roberts, H. H., and Carney, R. S. (1997). Evidence of episodic fluid, gas, and sediment venting on the northern gulf of Mexico continental slope. *Econ. Geol.* 92, 863–879. doi: 10.2113/gsecongeo.92.7-8.863
- Roberts, H. H., Coleman, J., Jesse Hunt, J., and Shedd, W. W. (2000). Surface amplitude mapping of 3-seismic for improved interpretations of seafloor geology and biology. *Gulf. Coast. Assoc. Geological. Soc. Trans.* 50, 495–504.
- Roberts, H. H., and Feng, D. (2013). “Carbonate precipitation at gulf of Mexico hydrocarbon seeps: an overview,” in *Hydrocarbon seepage: from source to surface*. Eds. M. Abrams, F. Aminzadeh, T. Berge, D. Connolly and G. O'Brien (SEG/AAPG Special Publication), 43–61. Available at: <https://pubs.geoscienceworld.org/seg/books/book/2106/chapterabstract/114897131/Carbonate-Precipitation-at-Gulf-of-Mexico?redirectedFrom=fulltext>.
- Roberts, H. H., Feng, D., and Joye, S. B. (2010). Cold-seep carbonates of the middle and lower continental slope, northern gulf of Mexico. *Deep-Sea. Res. Part II-Top. Stud. Oceanogr.* 57, 2040–2054. doi: 10.1016/j.dsr2.2010.09.003
- Roberts, H. H., Sassen, R., Carney, R., and Aharon, P. (1989). ¹³C-depleted authigenic carbonate buildups from hydrocarbon seeps, Louisiana continental slope. *Gulf. Coast. Assoc. Geological. Soc. Trans.* 39, 523–530.
- Sassen, R., Joye, S., Sweet, S. T., DeFreitas, D. A., Milkov, A. V., and MacDonald, I. R. (1999). Thermogenic gas hydrates and hydrocarbon gases in complex chemosynthetic communities, gulf of Mexico continental slope. *Org. Geochem.* 30, 485–497. doi: 10.1016/S0146-6380(99)00050-9
- Seni, S. J. (1992). Evolution of salt structures during burial of salt sheets on the slope, northern gulf of Mexico. *Mar. Pet. Geol.* 9, 452–468. doi: 10.1016/0264-8172(92)90054-I
- Smrzka, D., Zwicker, J., Klügel, A., Monien, P., Bach, W., Bohrmann, G., et al. (2016). Establishing criteria to distinguish oil-seep from methane-seep carbonates. *Geology* 44, 667–670. doi: 10.1130/G38029.1
- Suess, E. (2020). “Marine cold seeps: background and recent advances,” in *Hydrocarbons, oils and lipids: diversity, origin, chemistry and fate*. Ed. Wilkes, (Cham: Springer International Publishing), 747–767.
- Sun, Y., Gong, S., Li, N., Peckmann, J., Jin, M., Roberts, H. H., et al. (2020). A new approach to discern the hydrocarbon sources (oil vs. methane) of authigenic carbonates forming at marine seeps. *Mar. Pet. Geol.* 114, 104230. doi: 10.1016/j.marpetgeo.2020.104230
- Sun, Z., Wei, H., Zhang, X., Shang, L., Yin, X., Sun, Y., et al. (2015). A unique Fe-rich carbonate chimney associated with cold seeps in the northern Okinawa trough, East China Sea. *Deep-Sea. Res. Part I-Oceanogr. Res. Pap.* 95, 37–53. doi: 10.1016/j.dsr.2014.10.005
- Wang, M., Chen, T., Feng, D., Zhang, X., Li, T., Robinson, L. F., et al. (2022). Uranium-thorium isotope systematics of cold-seep carbonate and their constraints on geological methane leakage activities. *Geochim. Cosmochim. Acta* 320, 105–121. doi: 10.1016/j.gca.2021.12.016
- Watkins, J. M., Hunt, J. D., Ryerson, F. J., and DePaolo, D. J. (2014). The influence of temperature, pH, and growth rate on the δ¹⁸O composition of inorganically precipitated calcite. *Earth Planet. Sci. Lett.* 404, 332–343. doi: 10.1016/j.epsl.2014.07.036
- Whiticar, M. J. (1999). Carbon and hydrogen isotope systematics of bacterial formation and oxidation of methane. *Chem. Geol.* 161, 291–314. doi: 10.1016/S0009-2541(99)00092-3
- Whiticar, M. J., Faber, E., and Schoell, M. (1986). Biogenic methane formation in marine and fresh water environments: CO₂ reduction vs acetate fermentation – isotope evidence. *Geochim. Cosmochim. Acta* 50, 693–709. doi: 10.1016/0016-7037(86)90346-7
- Zhang, W., Chen, C., Su, P., Wan, Z., Huang, W., Shang, J., et al. (2023). Formation and implication of cold-seep carbonates in the southern south China Sea. *J. Asian Earth Sci.* 241, 105485. doi: 10.1016/j.jseas.2022.105485